Alkaloids from Lepidium meyenii (Maca), structural revision of macaridine and UPLC-MS/MS feature-based molecular networking

Alkaloids from *Lepidium meyenii* (Maca), structural revision of macaridine and UPLC-MS/MS feature-based molecular networking

Hien T. N. Le[1], Elias Van Roy[1], Ella Dendooven[1], Laura Peeters[1], Mart Theunis[1], Kenn Foubert[1], Luc Pieters[1], Emmy Tuenter[1]*

[1]Natural Products & Food Research and Analysis (NatuRA), Department of Pharmaceutical Sciences, University of Antwerp, Universiteitsplein 1, 2610, Antwerp, Belgium.

*lengocthaohien@gmail.com

Abstract

Lepidium meyenii Walp., known as Peruvian ginseng, is widely used in ethnomedicine. To date, *L. meyenii* is cultivated worldwide at high-altitude and is commonly used as a food supplement. However, its medicinal value is still controversial and its mechanism of action remains unknown, due to limited knowledge about the phytochemical constituents of this plant species. In this study, a multidisciplinary approach comprising conventional NMR- and HRMS-based structure elucidation, quantum mechanical calculation of NMR chemical shifts and UPLC-MS/MS feature-based molecular networking was applied to analyse the phytochemical profile of *L. meyenii*. In the current work, three previously undescribed imidazole alkaloids were identified using extensive spectroscopic techniques (HRMS, NMR), for which the names lepidiline E, F and G were adopted. In addition, two amidine alkaloids were reported, representing an undescribed class of alkaloids in *L. meyenii*, and 1,2,3,4-tetrahydro-*β*-carboline-3-carboxylic acid, a well-known *β*-carboline alkaloid, was also isolated from *L. meyenii* for the first time. Molecular networks of imidazole, amidine and *β*-carboline alkaloids in *L. meyenii* were constructed by the Global Natural Products Social Molecular Networking (GNPS) web platform, resulting in the tentative identification of three undescribed analogues. In addition, the structure of a previously reported compound named 'macaridine' was revised as macapyrrolin C based on density functional theory (DFT) calculations and comprehensive comparison of NMR data.

Key words:

Lepidium meyenii; Brassicaceae; lepidilines; amidine alkaloids; *β*-carboline alkaloids; density functional theory calculations; feature-based molecular networking

1. Introduction

Lepidium meyenii Walp. (Brassicaceae), known as "Maca", originates from the Central Andes in Peru. For many centuries, it has been cultivated because of the nutritional value of the root and for various medicinal purposes. Nowadays, it is widely sold worldwide as a dietary supplement (sometimes referred to as Peruvian Ginseng) to increase vitality and longevity, and most notably, to enhance fertility (Beharry and Heinrich, 2018). Characteristic constituents, which have been proposed as chemical markers, include polyunsaturated fatty acids (macaenes) and their amides (macamides) (Ganzera et al., 2002). In recent years, increasing attention has been paid to various other classes of constituents, such as β-carboline, pyrrole and imidazole alkaloids, glucosinolates, thioamides, hydantoins and thiohydantoins (Huang et al., 2018) (Carvalho and Ribeiro, 2019). According to Carvalho and Ribeiro (2019), 26 macamides and macaenes, 9 glucosinolates and 2 isothiocyanates were reported in the timeframe 2000-2018. In 2017-2018, a number of papers was published in which the alkaloid fraction was investigated in more detail, including pyrrole alkaloids (Zhou et al., 2017), thiohydantoin alkaloids (Zhou et al., 2017) (Yu et al., 2017), urea alkaloids (Kitamura et al., 2017), hexahydroimidazo[1,5-c]thiazole alkaloids (Zhou et al., 2017), hydantoin and thioamide alkaloids (Geng et al., 2018) (Tian et al., 2018). Not less than 26 alkaloids belonging to these skeleton types were reported; they can be considered as minor constituents because mostly large amounts of dried plant material (10-25 kg) were needed to obtain around 1-20 mg pure compound.

Although imidazole alkaloids, biogenetically derived from histidine, commonly exist in nature as tertiary alkaloids, two quaternary imidazole alkaloids, *i.e*. lepidilines A and B, were isolated from *L. meyenii* for the first time (Cui et al., 2003). Their atypical structures were elucidated by NMR spectroscopy and confirmed by X-ray crystallography. Afterwards, lepidilines C and D, which are methoxylated derivatives of lepidilines A and B, were reported by Jin et al. (2016). To the best of our knowledge, this type of quaternary imidazole alkaloid exists exclusively in *L. meyenii*, indicating that lepidilines can be used as chemical markers of this species. Interestingly, one of the main imidazole alkaloids, *i.e.* lepidiline A, was recently proposed as a potential active ingredient of Maca to enhance fertility (Cheng et al., 2020). This may indicate that the quaternary imidazole alkaloids could contribute to its sexual and fertility enhancing properties, together with the macamides and macaenes. Because of this unique quaternary imidazole moiety, it is important to further explore the chemical profile of the alkaloid fraction of *L. meyenii*. Therefore, in the present work, a detailed study of the alkaloidal profile of *L. meyenii* was carried out by means of NMR spectroscopy, UPLC-MS/MS and feature-based molecular networking, resulting in the isolation and identification of several previously undescribed imidazole alkaloids. In addition, the occurrence of amidine alkaloids was reported for the first time in Maca, and a structural revision of macaridine is proposed, based on density functional theory (DFT) calculations.

2. Results and discussion

2.1. Structure elucidation

Seven quaternary imidazole alkaloids were isolated from *L. meyenii*, three of which are reported here for the first time (**1** – **3**), whereas four were known (**4** – **7**) (Fig.1).

Comparison of the NMR spectra of compounds **4**, **5**, **6** and **7** with reported data confirmed their identity as lepidilines A-D, respectively (Cui et al., 2003; Jin et al., 2016). Compounds **4** and **5** showed NMR patterns typical for benzyl moieties, while compounds **6** and **7** contained both benzyl and methoxy-benzyl moieties. Compounds **4** and **5** produced simple ^{1}H NMR spectra with only a few (3-5) signals, but their symmetrical structures caused some difficulties in taking correct integrals. The only difference between compounds **4** and **5** is the methyl group at position 2 of compound **5**, which induces deshielding on the 4,5-Me groups. This is also observed for compounds **6** and **7**. Besides, the presence of a 4'-OMe group also produces significant changes in the UV spectra. The 4'-OMe functionality acts as an auxochrome attached to a benzene ring and causes a bathochromic shift from λ_{max} 230 to λ_{max} 274 nm. Therefore, compounds **4** and **5** only show an absorption maximum at λ_{max} 230 nm, but compounds **6** and **7** at both λ_{max} 230 and λ_{max} 274 nm. This was crucial for monitoring the separation of compounds **5** and **6** (the most difficult couple to separate) and for purification based on the UV spectra. In the HMBC spectra, key cross-peaks of the four compounds occur between H-1' and C-2, C-5, C-2', C-3' and C-7'; and between H-1" and C-2, C-4, C-2", C-3" and C-7". It should be noted that for compounds **4** and **6** the H-2 signal disappeared in the ^{1}H and 2D NMR spectra when $CDCl_3$ and CD_3OD were used as solvent. However, it could be observed in DMSO-d_6; the assignment of H-2 was further confirmed by HSQC (cross-peak between H-2 and C-2) and HMBC correlations (cross-peaks between H-2 and C-4, C-5, C-1' and C-2').

The NMR spectra of compound **1** showed the typical NMR pattern of a benzyl moiety, and those of compound **2** of a meta-methoxy-benzyl moiety as previously described for compounds **4 – 7**. Apart from this, other signals in their ^{1}H NMR spectra were identical. Hence, compounds **1** and **2** possess the same backbone, and compound **2** (yielding a molecular ion in MS at *m/z* 257.1653) bears an additional methoxy group compared to compound **1** (*m/z* 227.1553). In ^{1}H NMR, the benzyl methylenes of compounds **1** and **2** were observed within the same chemical shift range (~5.35-5.45 ppm) as compounds **4** – **7**, which are imidazole alkaloids. Therefore, it was hypothesized that compounds **1** and **2** also possessed an imidazole ring. Nevertheless, in contrast to compounds **4** – **7**, compounds **1** and **2** contained a bicyclic structure, consisting of an imidazole ring fused to a cyclopentane ring, based on the following observations: (1) three -CH_2- functionalities were evident from the DEPT-135 spectrum; (2) the -CH_2-CH_2-CH_2- moiety was confirmed by COSY correlations and by the coupling pattern in ^{1}H NMR, i.e. a triplet (J ~ 7.5 Hz), a quintet (J ~ 7.5 Hz) and a triplet (J ~ 7.5 Hz), each with an integration of two; (3) all three -CH_2- moieties showed

HMBC correlations with C-2 of the imidazole ring, indicating a 2- or 3-bond distance; (4) one head of the -CH_2-CH_2-CH_2- functionality is connected to a nitrogen atom (N-3), as one -CH_2- has a remarkably more downfield shift in ^{1}H and ^{13}C NMR (H-8, ~4.20 ppm; C-8, ~47.0 ppm) than the other two -CH_2- units, due to its connection to an electronegative element; this was further confirmed by a HMBC correlation between H-8 and C-4; (5) the other head of the -CH_2-CH_2-CH_2- functionality is linked to C-2, as the chemical shift of C-2 is 151.6 ppm, indicating it must be substituted. Finally, the correct assignment of 4-Me and 5-Me was deduced from NOE effects between H-1' and 5-Me and between H-8 and 4-Me. All NMR assignments are listed in Table 1, and key correlations are shown in Fig. 2. The structures proposed for compounds **1** and **2** were confirmed by HRMS. In UV spectroscopy, compound **1** showed a λ_{max} at 230 nm and compound **2** at both 230 and 274 nm. Compounds **1** and **2** are reported for the first time, and the names lepidiline E and F, respectively, were adopted.

Compound **3** was isolated as a mixture with compound **1**. Thus, NMR analysis of the mixture was carried out, of which compound **1** was the major and compound **3** the minor compound (ratio 5:1). Similar to compound **1**, the NMR pattern of a benzyl moiety was observed for compound **3** and its benzyl methylene resonated at 5.37 ppm, suggesting the possible presence of an imidazole ring. Structure elucidation of compound **3** started with the HMBC correlations of H-1' (benzyl methylene), since this peak did not overlap with proton signals of compound **1**. H-1' correlated with carbons at 128.7 and 134.5 ppm, similar to H-1' and H-1" of compound **4** and H-1" of compound **6**. Therefore, it was deduced that compound **3** contains an imidazole ring bearing a benzyl group on one of its two nitrogen atoms. The ^{13}C NMR signal at 128.7 ppm was then assigned to C-3', C-7' and C-4; the signal at 134.5 ppm was assigned to C-2, indicating that this position is not substituted. Two methyl groups attached to the imidazole ring were assigned as follows: (1) a methyl group was observed in the ^{1}H NMR spectrum at 2.31 ppm with an integral of three; (2) a second methyl group of compound **3** was observed at 2.19 ppm, but overlapped with the 5-Me signal of compound **1**, as indicated by its integral. The peak area of this signal equals the sum of the peak areas of two methyl groups at 2.25 ppm (4-Me of compound **1**) and 2.31 ppm (a methyl-group of compound **3**). Finally, it was supported by a HMBC correlation with the ^{13}C NMR signal at 128.7 ppm (C-4). The correct assignment of these two methyl groups was confirmed by NOE effects. Likewise, the ethyl group attached to a nitrogen of the imidazole ring was elucidated as follows: (1) a triplet at 1.52 ppm with an integral of three, which showed a COSY correlation with a signal at 4.20 ppm, indicating an overlap with a signal of compound **1** with the same chemical shift; (2) the peak area of the signal at 4.20 ppm equals the sum of the peak areas of a methylene of the major compound **1** and a methylene of the minor compound **3**; (3) HMBC cross-peaks between the methylene of the minor compound **1** with ^{13}C NMR signals at 134.5 ppm (C-2), 128.7 ppm (C-5) and most importantly, at 15.0 ppm (CH_3 of the ethyl group). Taken altogether, compound **3** was identified as 1-benzyl-3-ethyl-4,5-dimethylimidazolium. NMR assignments are listed in Table 1, and key

correlations are shown in Fig. 2. HRESIMS yielded a molecular ion at *m/z* 215.1550 $[M]^+$, confirming the chemical formula $C_{14}H_{19}N_2$ of the proposed structure. As a remark, H-2 was only observed in DMSO-d_6 at 9.71 ppm, but not observed in MeOH-d_4. Compound **3** is reported for the first time, and the name lepidiline G was adopted.

The NMR spectra of compounds **9** and **10** again indicated the presence of two benzyl moieties. Their elemental composition was established as $C_{16}H_{18}N_2$ (*m/z* 239.1549, $[M+H]^+$) and $C_{15}H_{16}N_2$ (*m/z* 225.1402, $[M+H]^+$), respectively, based on HRESIMS. Since the two benzyl moieties alone already account for 182 Da, along with 28 Da for two nitrogen atoms, the remaining part of the structure of compounds **9** and **10** must correspond to 27 and 13 Da, respectively, which indicated the presence of a -C-CH_3 and a -CH- moiety, respectively. In the HMBC spectra, cross-peaks of the benzyl methylenes (H-1' and H-1") with deshielded carbon signals around 163-169 ppm in ^{13}C NMR inferred that these carbons are positioned between the two nitrogen atoms, forming an -N-C=N- backbone. This is in agreement with several synthetic amidine analogues reported in literature (Maccallini et al., 2015). Therefore, the structure of compound **9** was elucidated as an acetamidine derivative, i.e. *N,N'*-dibenzylacetamidine, and compound **10** as a formamidine derivative, i.e. *N,N'*-dibenzylformamidine (Fig. 1). In organic chemistry, amidine analogues are quite common, but to the best of our knowledge, this is the first time amidine alkaloids are reported as plant-derived natural products.

In literature, considerable efforts have been made to clarify the chemistry of acyclic amidines, and in non-aqueous solutions, amidines exhibit tautomerism with respect to the position of the double bond in the -N-C=N- moiety and *Z-E* isomerism with respect to the C=N double bond (Minkin and Mikhailov, 2010). As for compounds **9** and **10**, it appears that *Z-E* isomerism was observed when changing the solvent from DMSO-d_6 to $CDCl_3$. In DMSO-d_6, only the *E*-isomer exists, as the *E*-isomer is energetically preferred over the *Z*-isomer (mainly due to the steric effect of the benzyl moieties). This phenomenon in $CDCl_3$ or $CHCl_3$ was previously described for amidine derivatives (Minkin and Mikhailov, 2010). However, in-depth research on tautomerism and isomerism is beyond the scope of this study, and we only report the phenomena observed according to the two solvents used: $CDCl_3$ and DMSO-d_6. As for compound **10**, the ratio between the two isomers is approximately 1.5:1 in $CDCl_3$. The ^1H NMR spectrum of compound **9** in $CDCl_3$ showed the presence of at least three isomers, and we assume that the most abundant isomer is the one observed in DMSO-d_6. In COSY, cross-peaks between H-1" and 3-NH were clearly observed. It can be noticed that the chemical shift of 3-NH varies for the different isomers from 8.85 to 11.05 ppm, of which the most downfield 3-NH belongs to the most abundant isomer. Table 2 shows the NMR assignments for the major isomer of compound **9** and two isomers of compound **10** in $CDCl_3$.

β-Carboline alkaloids, isolated from several plant genera and animals, were reported to exhibit multiple pharmacological effects, including neuro-pharmacological and antitumoural activities. However, some *β*-

carbolines showed mutagenic and carcinogenic properties (Cao et al., 2007). Therefore, it is crucial to check their presence in a common food supplement like *L. meyenii*. Until now, only (1*R*,3*S*)-1-methyl-1,2,3,4-tetrahydro-*β*-carboline-3-carboxylic acid (MTCA), which is a well-known *β*-carboline alkaloid (Gutsche and Herderich, 1997) was isolated from a butanolic extract of *L. meyenii*. Compound **11** was identified as 1,2,3,4-tetrahydro-*β*-carboline-3-carboxylic acid (Fig. 1), showing resemblance to MTCA. Briefly, the ^{1}H NMR spectrum of compound **11** showed NMR signals typical for an indole moiety: (1) four adjacent aromatic hydrogens (H-5, H-6, H-7 and H-8) appeared as a doublet (*J*=7.8 Hz), a doublet of triplets (*J*=7.8, 1.5 Hz), a doublet of triplets (*J*=7.8, 1.5 Hz) and a doublet (*J*=7.8 Hz), respectively; (2) in DMSO-d_6, the NH signal of the indole nucleus was highly deshielded and resonated at 10.87 ppm (9-NH); (3) HMBC correlations of the 9-NH with aromatic carbons (C-4a, C-4b, C-8a and C-9a) were observed. Next, two AB systems with a large coupling constant of 15-16 Hz indicated two methylene functionalities attached to the indole nucleus (1-CH_2- and 4-CH_2-), constituting a 4a, 9a-disubstituted pyrrole moiety. The 4-CH_2- group correlated with H-3 (3.54 ppm) in COSY, and H-3 correlated with the carboxyl-group at 170.5 ppm in the HMBC spectrum. Notably, hydrogen signals of the carboxyl-group and 2-NH were not observed in DMSO-d_6. Although this compound is known, this was the first time it was isolated from *L. meyenii*.

2.2. Structural revision of 'macaridine'

Compound **8** surprisingly showed ^{1}H and ^{13}C NMR chemical shift values similar to two compounds previously reported by Muhammad et al. (2002) and Zhou et al. (2018) for macaridine and macapyrrolin C (see Table 3 and Fig.3), respectively, which both have a molecular formula $C_{13}H_{13}NO_2$ (Muhammad et al., 2002; Zhou et al., 2018). The only small difference in reported spectroscopic data is the UV absorption: 'macaridine' showed a λ_{max} in methanol at 208, 255 and 294 nm, while for macapyrrolin C only a λ_{max} in methanol at 292 nm was reported. In our study, we followed the isolation procedure described by Muhammad et al. (2002) with the aim of isolating macaridine. However, on the basis of extensive 2D NMR analysis, the structure of compound **8** was elucidated as macapyrrolin C. In the 'macaridine' structure, HMBC correlations are expected between H-8/C-8 (δ_H 5.73/ δ_C 48.9) and H-2/C-2 (δ_H 4.54/ δ_C 57.0). However, surprisingly, Muhammad et al. (2002) did not observe such HMBC correlations, in spite of the favorable three-bond distance between positions 2 and 8 in the proposed structure. Nevertheless, absence of this HMBC correlation would be more likely in case of a four-bond distance between these specific signals, as would be the case for H-1'/C-1' and -CH_2- of 5-CH_2OH (δ_H 5.76/ δ_C 49.0 and δ_H 4.57/ δ_C 57.1, respectively) in macapyrrolin C. Apart from that, Zhou et al. (2018) reported three pyrrole alkaloids from *L. meyenii*, i.e. macapyrrolins A-C, while no other macaridine-like analogues were reported so far.

Over the last decades, the calculation of nuclear magnetic shielding constants by the Density Functional Theory (DFT) has been developed and widely applied to support structure elucidation and to predict relative configurations (Lodewyk et al., 2012). In the current study, DFT calculations were performed for the two

structures, ‘macaridine’ and macapyrrolin C, in order to obtain additional proof for the structural revision of ‘macaridine’. Since the two structures are highly different, the DFT calculation can be expected to match with only one of the two. The mPW1PW91 functional, which has been reported as one of the best overall functionals for computing ^{13}C NMR chemical shifts, was used with a triple-ζ Pople’s basis set 6-311+G(2d,p) to calculate quantitative computed data (Jensen, 2008; Ermanis et al., 2017). Consequently, as can be seen in Table 3, calculated chemical shifts of macapyrrolin C are in complete agreement with the experimental data with a corrected-mean absolute error (CMAE) of 0.183 ppm for hydrogen shifts and 1.008 ppm for carbon shifts. The deviations for ‘macaridine” are much more pronounced. The calculated data also explain the deshielding effect observed for H-1’ (δ_H 5.76) and C-1’ (δ_C 49.0) of macapyrrolin C, which is caused by attachment to the nitrogen of the pyrrole ring, but which is not the case for ‘macaridine’. Therefore, the structure of ‘macaridine’ is to be revised as macapyrrolin C. Detailed information about all contributing conformers subjected to DFT calculations can be found as Supporting Information.

2.3. Molecular networking and metabolomics analysis

In nature, the quaternary imidazole alkaloids represent a unique class of compounds reported exclusively in *L. meyenii*. In order to gain more insight in the compositional profile of this class of compounds, a molecular network-guided approach was followed. Fig. 4 shows the molecular network containing the imidazole alkaloids obtained in the present work, i.e. compounds **1** – **7** (nodes (6), (16), (3), (24), (29), (36) and (40), respectively).

Known compounds are shown as orange nodes, unknown compounds as grey nodes and tentatively identified compounds as grey nodes with black borders. The node size correlates with the relative abundance of each feature. Since lepidilines A – F are quaternary alkaloids that can be detected in positive ion mode without the need of ionisation in the ion source, and since their structures are rather similar, their peak intensity shows a more or less linear correlation to their concentration. Therefore, the peak intensities of the lepidiline signals were used to estimate the ratios of lepidilines in our samples. Hence, the node sizes of the lepidilines A-F were adjusted according to their relative intensities determined in the CH_2Cl_2 (I) fraction of procedure 1 (see Fig. S62), which were 7.14+E5, 8.88+E5, 3.83+E5, 3.06+E5, 1.44+E5, 2.29+E4 and 2.60+E4, respectively. It is clear that lepidilines A and B are the major imidazole alkaloids, followed by lepidilines C, D and E. Lepidilines F and G are found in levels approximately ten-fold less than lepidilines C, D and E, and twenty-fold less than lepidilines A and B.

Interestingly, two amidine alkaloids (nodes (5) and (10)) are also present in the cluster, but are found further away from the region of the known imidazole alkaloids. Most probably, this cluster contains compounds with a -N=C-N- moiety, including imidazole, amidine and possibly other unknown scaffolds.

Another noteworthy point is the fact that there are three *m/z* values (227.15, 215.15 and 239.15) which were reported before in several HRMS-based metabolomics studies of *L. meyenii*. However, the structures of our

purified compounds with corresponding *m/z* values (compounds **1**, **3** and **9**, respectively) are not in agreement with the previously proposed structures. Zhou et al. (2017) suggested that the product with *m/z* 227.15 corresponded to 1-dibenzyl-2-propane-4,5-dimethylimidalium, but this chemical name is incorrect, and instead should be 1-benzyl-2-propane-4,5-dimethylimidazolium, if the compound would exist. Furthermore, this chemical name was assigned to two different *m/z* values: 227.15 and 229.16, which were different peaks eluting at different retention times (Zhou et al., 2017). Unfortunately, this misinterpretation was restated by Tafuri et al. (2019). Concerning the product with *m/z* 215.15, Zhou et al. (2017) and Geng et al. (2020) proposed the structure of 1-benzyl-2-ethyl-4,5-dimethylimidazolium, which was also erroneously named as 1-dibenzyl-2-ethyl-4,5-dimethylimidazolium. Apart from these mistakes in chemical names, it can be deduced that these studies did not consider the possibility of substitution on both N-1 and N-3, and therefore, a substituent was erroneously located in position C-2 instead of N-3. Since the present study describes the presence of amidine alkaloids in *L. meyenii* for the first time, misinterpretations in previously published metabolomics research for this class of compounds were inevitable. For instance, the ion with *m/z* 239.15 was proposed to correspond to an imidazole alkaloid by Zhou et al. (2017).

As stated by the GNPS platform, molecular networks are built based on similarities between MS fragmentation data of all compounds. Therefore, compounds within close proximity are expected to show the highest structural similarities. Three grey nodes with black borders (13), (46) and (49) correspond to *m/z* values of 245.1654, 337.1913 and 351.2079, respectively. Node (13) is one of the first neighbors of lepidiline F, while nodes (46) and (49) share lepidilines C and D as first neighbors. Based on the mass difference of 30 Da observed between three couples (245.1654 and 215.1550 (lepidiline F), 337.1913 and 307.1806 (lepidiline C), 351.2079 and 321.1968 (lepidiline D)), the signal at *m/z* 245.1654 likely represents a methoxylated derivative of lepidiline F, the signal at *m/z* 337.1913 a methoxylated derivative of lepidiline C, and the signal at *m/z* 351.2079 a methoxylated derivative of lepidiline D. The position of the additional -OMe groups can be deduced based on knowledge about the -OMe position of the imidazole alkaloids identified in this study: lepidilines C, D and F possess only one -OMe group, which is meta-oriented. Furthermore, the effect of –OMe substitution on the retention properties on a RP-C18 column was assessed. It was observed that compounds with a -OMe group attached to a benzyl moiety are more strongly retained on the RP-C18 stationary phase (Fig. S62-S65): lepidiline C elutes slower than lepidiline A; lepidiline D is more retained than lepidiline B; and lepidiline F elutes slower than lepidiline E; a similar behavior was observed for products with *m/z* values 245.1654, 337.1913 and 351.2079. Thus, we tentatively identified the structures corresponding to these three *m/z* values as 3-ethyl-1-(3'-methoxybenzyl)-4,5-dimethyl-imidazolium for *m/z* 245.1654; 1,3-bis(3'-methoxybenzyl)-4,5-dimethyl-imidazolium for *m/z* 337.1913; and 1,3-bis(3'-methoxybenzyl)-2,4,5-trimethyl-imidazolium for *m/z* 351.2079 (Fig. 5). Finally, due to co-elution, fragmentation patterns of these compounds were mixed with those of other compounds in the MSe

spectra. Therefore, we performed MRM scans to confirm specific fragments in positive ion mode, and three fragmentation reactions were set for each parent ion (Fig. 5).

3. Conclusion

In this study, the alkaloid fraction of *L. meyenii* was explored. Three undescribed imidazole alkaloids were identified, for which the names lepidiline E, F and G were adopted, along with three tentatively identified imidazole derivatives. Amidine alkaloids were also described for the first time in this species. UPLC-HRMS-based molecular networking indicated the presence of imidazole, amidine and *β*-carboline alkaloids. Thorough comparison of our findings and previous profiling studies pointed out several misinterpretations with regard to the imidazole alkaloids. From our point of view, it is crucial to restate that isolation and structure elucidation by NMR is the key to undoubtedly identify phytochemical constituents. To avoid misinterpretations, care should be taken in metabolomics research based on HRMS data, and tentative identification should only be carried out in combination with thorough proof.

Furthermore, macapyrrolin C was purified and was used as a reference to revise the structure of previously reported 'macaridine'. Based on the comprehensive comparison of NMR data and DFT calculations, it was confirmed that the structure reported for 'macaridine' should be revised as macapyrrolin C.

4. Experimental

4.1. General experimental procedures

All solvents, including methanol, ethanol and dichloromethane were purchased from Acros Organics (Geel, Belgium) or from Fisher Scientific (Loughborough, UK) and were analytical grade. Reagents, including TLC spraying reagents: ammonia 25% (NH_4OH 25%), formic acid (FA 98%), MS-grade formic acid (FA 99%), acetic acid (AA 98%), hydrochloric acid 25% (HCl 25%), potassium iodide (KI 99%), ammonium acetate (NH_4Ac 98%), diethylamine (DEA 99%) and bismuth (III) nitrate ($Bi(NO_3)_3$ 99.5%) were purchased from either Acros Organics (Geel, Belgium), Sigma-Aldrich (St. Louis, MO, USA) or Merck (Darmstadt, Germany). Solvents used for HPLC and UPLC, i.e. methanol (MeOH) and acetonitrile (ACN) were HPLC and UPLC grade and were purchased from Fisher Scientific (Loughborough, UK) and Biosolve BV (Valkenswaard, the Netherlands), respectively. Water was dispensed and filtered by a Direct-Pure Up Ultrapure and RO water system (Rephile Bioscience, Belgium).

TLC was performed on pre-coated silica gel F254 plates (Merck, Darmstadt, Germany), and the bands were observed under UV light (254 and 366 nm), as well as under visible light after spraying with the Dragendorff reagent. Dragendorff reagent was prepared by combining a mixture A and a solution B. Mixture A was prepared by suspending 0.85 g of bismuth subnitrate ($Bi_5O(OH)_9(NO_3)_4$) in 40 mL of water and 10 mL of glacial acetic acid. Solution B was prepared by dissolving 8 g of potassium iodide (KI) in 20 mL of water.

Flash chromatography was performed on a Grace Reveleris X2 system (Columbia, MD, USA) using the Reveleris Navigator™ software. The system was equipped with a binary pump, a UV detector, an evaporative light scattering detector and a fraction collector.

HPLC analysis was performed on an Agilent 1200 series HPLC-DAD system (Agilent Technologies, Santa Clara, USA) with OpenLAB software version A.01.05. A Phenomenex Kinetex EVO C18 column (250 x 4.6 mm, 5 µm) was used for analytical purposes and a Phenomenex Kinetex EVO C18 column (250 x 10.0 mm, 5 µm) for semi-preparative purification (Phenomenex, Utrecht, the Netherlands).

UPLC-MS and UPLC-MS/MS analyses were conducted on two different systems: UPLC-TQD-MS and UPLC–QTOF-MS/MS (Xevo G2-XS QToF mass spectrometer), both comprising an Acquity UPLC (Waters Corporation, Milford, MA, USA) and using MassLynx software version 4.1. A Phenomenex Kinetex EVO C18 column (100 x 2.1 mm, 2.6 µm) was used.

Optical rotations were measured on a Jasco P-2000 spectropolarimeter (Easton, MD, USA) equipped with the Spectra Manager™ software.

1D and 2D NMR spectra were either recorded on a DRX-400 or an Avance Nanobay III NMR instrument (Bruker BioSpin, Rheinstetten, Germany), both operating at 400 MHz for ^{1}H and 100 MHz for ^{13}C-analysis. NMR data processing was performed using TopSpin software version 4.0.6 from Bruker. For NMR experiments, methanol-d_4 (CD_3OD - 99.8% D), chloroform-*d* ($CDCl_3$ - 99.8% D) and dimethyl sulfoxide-d_6 (99.9% D) were purchased from Sigma-Aldrich (Merck, Germany).

4.2. Plant material

Two batches of plant material were purchased from two suppliers: (1) 2 kg hydroglycerin organic flour of the roots of *Lepidium meyenii* Walp. (Brassicaceae), drug/extract ratio 4:1, batch number 0001-29708/18 supplied by Soria Bel N.V. (Ichtegem, Belgium) and (2) 1 kg of "Bio-Maca Pulver" (root powder), batch number 87619, supplied by Herbis Natura GmbH (Berlin, Germany).

4.3. Extraction and isolation

Two different isolation procedures were used for the two batches of plant material: the first one followed a general fractionation scheme, the second one was more dedicated.

4.3.1. Procedure 1 (applied to the first batch of plant material):

Root flour (2 kg) was macerated and percolated with approximately 25 L of 80% ethanol, filtered and dried under reduced pressure. Next, liquid-liquid partition was applied in order to obtain an alkaloid-rich fraction. Briefly, crude extract was suspended in water and was acidified with 10% HCl to a pH < 3 before performing liquid-liquid partition with CH_2Cl_2 (I). Next, the pH of the acidified phase was increased to a value ≥ 9 by adding NH_4OH (25%), followed by a second liquid-liquid partition with CH_2Cl_2 (II). In this way, three fractions (CH_2Cl_2 (I), CH_2Cl_2 (II) and a residual aqueous fraction) were obtained and were examined by TLC with a mobile phase of EtOAc/MeOH/NH_4OH/H_2O (80:20:1:1). Observation of the TLC

plates after spraying with the Dragendorff reagent indicated that the majority of alkaloids was present in the CH_2Cl_2 (I) fraction (16.2 g).

To confirm the presence of alkaloids in the CH_2Cl_2 (I) fraction, UPLC-TQD-MS analysis in positive ionization mode was performed using either a general MS scan detection method or a Selected Ion Recording (SIR). The latter aimed at the specific identification of the four reported major alkaloids from *L. meyenii*: lepidilines A-D and *m/z* values used in our method were derived from earlier studies performed by Cui et al. (2003) and Jin et al. (2016): *m/z* values of 277, 291, 307 and 321 (all $[M^+]$) were set for the identification of 1,3-dibenzyl-4,5-dimethylimidazolium chloride (lepidiline A), 1,3-dibenzyl-2,4,5-trimethylimidazolium chloride (lepidiline B), 3-benzyl-1-(3-methoxybenzyl)-4,5-dimethylimidazolium chloride (lepidiline C) and 3-benzyl-1-(3-methoxybenzyl)-2,4,5-trimethylimidazolium chloride (lepidiline D), respectively. As a result, the presence of lepidilines A-D in the CH_2Cl_2 (I) fraction was confirmed by SIR, while the MS scan analysis revealed the presence of several other unknown constituents. Next, the CH_2Cl_2 (I) fraction was further fractionated using a Diaion® HP-20 column. The column was sequentially eluted with MeOH/H_2O (10:90), MeOH/H_2O/AA (40:60:0.5) and MeOH/H_2O/AA (50:50:0.5). Fractions of 250 mL each were collected and concentrated under reduced pressure followed by freeze-drying. Fractions showing identical spots on TLC were combined. This resulted in four subfractions, namely OC1, OC2, OC3 and OC4. UPLC-TQD-MS profiling was carried out on the four subfractions using the aforementioned method and lepidilines A-D were all found to be present in fractions OC3 and OC4, while fractions OC1 and OC2 mainly contained unknown *m/z* values.

Based on these results, further fractionation by flash chromatography was performed. All four fractions OC1 (41 mg), OC2 (45 mg), OC3 (659 mg) and OC4 (342 mg) were fractionated using Claricep™ C-series cartridges containing 12 g deactivated silica gel (40-60 µm). Solvents were CH_2Cl_2 (A) and MeOH + 0.1% AA (B) and the flow rate was 27 mL/min. The gradient used was: 0-5 min (0% B), 45-47 min (40% B), 50-60 min (100% B), while the gradient was halted during elution of detected compounds. The UV detector was set at 230 and 274 nm. After flash chromatography, fractions were combined based on the resulting chromatograms and on TLC analysis and were profiled by UPLC-TQD-MS.

From fraction OC1, a mixture of two compounds was obtained with *m/z* values of 227 (major compound) and 215 (minor compound) in positive ionization mode. However, the amount of the mixture was only 2 mg, and therefore, further analysis by NMR was carried out on the mixture as such with the aim of identifying both compounds. From fraction OC2, subfraction H3 was derived, containing two main constituents with *m/z* values of 227 and 257 in positive ionization mode. From subfractions OC3 and OC4, five new subfractions (FC1-FC5) were obtained, of which subfractions FC1 and FC2 were selected for further purification.

Semi-preparative HPLC-DAD with manual collection was performed for isolation of pure compounds from the fractions FC1, FC2 and H3. More specifically, the preparative method for fractions FC1 and FC2 was: (1) sample concentration: 1 mg/mL in water; (2) injection volume: 600 µL; (3) solvent A: H_2O/NH_4Ac/FA (100:0.5:0.3, v/v) and solvent B: MeOH/NH_4Ac/FA (100:0.5:0.3, v/v) (NH_4Ac was prepared as a 20 µM solution); (4) gradient: 0-5 min (50% B), 14 min (56% B), 16 min (90% B), 18-23 min (50% B); (5) UV detection: 230 and 274 nm; (6) flow rate: 3 mL/min. To be noticed, lepidilines B and C co-eluted during earlier analysis, but the addition of NH_4Ac resulted in baseline separation of these two alkaloids. The HPLC conditions for fraction H3 were: (1) sample concentration: 5 mg/mL in MeOH; (2) injection volume: 100 µL; (3) solvent A: H_2O/FA/DEA (100:0.5:0.3, v/v) and solvent B: ACN/MeOH/FA/DEA (80:20:0.5:0.3, v/v); (4) gradient: 0-10 min (25% B), 15 min (38% B), 20-23 min (90% B), 25-30 min (25% B); (5) UV detection: 230 and 274 nm; (6) flow rate: 3 mL/min. Finally, to remove the diethylamine formate, solid-phase extraction with a Chromabond® C18 ec (500 mg, 6 mL) column (Macherey-Nagel, Düren, Germany) was carried out. Each sample was dissolved in water, loaded on an activated column and subsequently, the column was rinsed with 4 column volumes of water to remove the salt. In a next step, the column was rinsed with 3 column volumes of MeOH to elute the purified alkaloids.

Lepidilines E and F (compounds **1** and **2**) were purified by semi-preparative HPLC-DAD of fraction H3. Lepidilines E and G (compounds **1** and **3**) were isolated from fraction OC1 by flash chromatography as a mixture, as previously mentioned. Lepidilines A-D (compounds **4**-**7**) were isolated by semi-preparative HPLC-DAD from fractions FC1 and FC2.

4.3.2. Procedure 2 (applied to the second batch of plant material):

Similar to the first procedure, root powder (1 kg) was macerated and percolated with approximately 15 L of 80% ethanol, filtered and dried under reduced pressure to obtain a crude extract. However, taking into consideration the publication of Muhammad et al. (2002) and the chemical nature of the targeted compounds, the partitioning procedure was modified in order to optimize the isolation of the lepidilines, macaridine and (1R,3S)-1-methyl-1,2,3,4-tetrahydro-*β*-carboline-3-carboxylic acid (MTCA) as follows: (1) First, the crude extract was suspended in water and partitioned with CH_2Cl_2 (I), (2) Second, the water phase was acidified to pH < 3 and was partitioned with CH_2Cl_2 (II), (3) Finally, the acidified water phase was partitioned with *n*-butanol (Muhammad et al., 2002).

The CH_2Cl_2 (I) extract (12 g) was fractionated by flash chromatography using a Claricep™ C-series cartridge containing 40 g deactivated silica gel (40-60 µm). Briefly, settings of the flash system were as follows: (1) solvents: CH_2Cl_2 (A), MeOH + 0.5% AA (B); (2) flow rate: 30 mL/min; (3) gradient: 0-5 min (0% B), 50-55 min (60% B), 60-70 min (100% B) and the gradient was halted during elution of detected compounds; (4) UV detection: 230 and 274 nm. The *n*-butanol extract (15 g) was fractionated using an MCI column (200 g) and a gradient of increasing MeOH:H_2O ratios. In both cases, collected fractions were

combined based on TLC analysis, resulting in 15 subfractions originating from the CH_2Cl_2 (I) extract and 40 subfractions derived from the n-BuOH extract. All subfractions were analyzed by UPLC-TQD-MS for the identification of lepidilines, macaridine and MTCA. The UPLC-TQD-MS conditions were identical to those described in procedure 1, but for SIR, *m/z* values of 216.1 $[M+H]^+$ and 231.2 $[M+H]^+$, were added for the identification of macaridine and MTCA in positive ionization mode, respectively (Muhammad et al., 2002). This analysis revealed that the lepidilines, 'macaridine' and MTCA were all present in different fractions.

The isolation of lepidilines A, B, C, D and E was repeated according to the methods described in procedure 1, in order to obtain a higher amount of each.

Isolation of 'macaridine' was carried out by preparative HPLC-DAD of fraction CH_2Cl_2 (I), using the following conditions: (1) sample concentration: 10 mg/mL in MeOH; (2) injection volume: 60 µL; (3) solvent A: H_2O + 0.1% FA and solvent B: ACN + 0.1% FA (v/v); (4) gradient: 0-5 min (25% B), 20 min (40% B), 28 min (72% B), 30-32 min (90% B) and 34-38 min (25% B); (5) UV detection: 210, 274 and 294 nm; (6) flow rate: 3 mL/min.

Semi-preparative HPLC-DAD was performed on fraction *n*-BuOH-11, the fraction presumably containing MTCA. The conditions were as follows: (1) sample concentration: 5 mg/mL in MeOH; (2) injection volume: 120 µL; (3) solvent A: H_2O and solvent B: ACN/MeOH – 4/6 (v/v); (4) gradient: 0-5 min (10% B), 20 min (25% B), 23 min (100% B) and 25-30 min (10% B); (5) UV detection: 210 and 254 nm; (6) flow rate: 3 mL/min.

Accurate mass measurements were performed for all isolated compounds **1-11**. 1D and 2D NMR spectra were recorded for structure elucidation of all compounds.

4.3.3. Spectroscopic data

Lepidiline E (**1**)

Yellow amorphous powder (3 mg); UV λ_{max} 230 nm; ^1H and ^{13}C NMR (CD_3OD, 400 and 100 MHz): see Table 1; Positive HRESIMS *m/z* 227.1552 $[M]^+$ (calcd for $C_{15}H_{19}N_2$, 227.1548)

Lepidiline F (**2**)

Yellow amorphous powder (< 1 mg); UV λ_{max} 230, 274 nm; ^1H and ^{13}C NMR (CD_3OD, 400 and 100 MHz): see Table 1; Positive HRESIMS *m/z* 257.1656 $[M]^+$ (calcd for $C_{16}H_{21}N_2O$, 257.1654)

Lepidiline G (**3**)

Yellow amorphous powder (< 1 mg); UV λ_{max} 230 nm; ^1H and ^{13}C NMR (CD_3OD, 400 and 100 MHz): see Table 1; ^1H NMR (DMSO-d_6, 400 and 100 MHz): δ_H 9.71 (s, H-2), 7.29-7.41 (m, overlapped, H-3', H-4', H-5', H-6', H-7', H-3", H-4", H-5", H-6", H-7"), 5.44 (s, H-1'), 4.16 (H-1"), 2.23 (s, 4-Me), 2.11 (overlapped, 5-Me), 1.41 (overlapped, H-2"); Positive HRESIMS *m/z* 215.1551 $[M]^+$ (calcd for $C_{14}H_{19}N_2$, 215.1548)

N,N'-dibenzylacetamidine (**9**)

Yellow amorphous powder (1.5 mg); UV λ_{max} 230, 256 nm; ^{1}H and ^{13}C NMR ($CDCl_3$, 400 and 100 MHz): see Table 2; ^{1}H and ^{13}C NMR (DMSO-*d6*, 400 and 100 MHz): δ_H 7.35-7.40 (overlapped, H-4', H-5', H-6', H-4", H-5", H-6"), 7.28-7.30 (overlapped, H-3', H-7', H-3", H-7"); 4.56 (s, H-1'), 4.53 (s, H-1"), 2.25 (s, 2-Me); δ_C 164.3 (C-2), 128.9 (C-4', C-5', C-6', C-4", C-5", C-6"), 127.4 (C-3', C-7', C-3", C-7"), 47.0 (C-1'), 45.4 (C-1"), 17.3 (2-Me); Positive HRESIMS *m/z* 239.1549 $[M+H]^+$ (calcd for $C_{16}H_{19}N_2$, 239.1548)

N,N'-dibenzylformamidine (**10**)

Yellow amorphous powder (1 mg); UV λ_{max} 230, 256 nm; ^{1}H and ^{13}C NMR ($CDCl_3$, 400 and 100 MHz): see Table 2; ^{1}H and ^{13}C NMR (DMSO-d_6, 400 and 100 MHz): δ_H 7.37-7.41 (overlapped, H-4', H-5', H-6'), 7.32-7.39 (overlapped, H-2, H-3", H-4", H-5", H-6", H-7"); 4.46 (s, H-1'), 3.77 (s, H-1"); δ_C 165.9 (C-2), 136.0 (C-2'), 134.9 (C-2"), 129.2 (C-3", C-7"), 129.0 (C-4', C-5', C-6', C-4", C-5", C-6"), 128.2 (C-3', C-7'), 45.6 (C-1'), 38.8 (C-1"); Positive HRESIMS *m/z* 225.1402 $[M+H]^+$ (calcd for $C_{15}H_{17}N_2$, 225.1392)

Lepidilines A-D (**4**, **5**, **6**, **7**), macapyrrolin C (**8**), 1,2,3,4-tetrahydro-*β*-carboline-3-carboxylic acid (**11**): see as Supporting information

4.4. DFT calculations

Input 2D and 3D structures were generated by ChemDraw 19.1 and Chem3D 19.1 software, respectively. Monte Carlo conformational search was performed by PCMODEL (version 10.0) using Merck Molecular Force Field (MMFF94) applying 8 and 7 kcal.mol^{-1} energy windows for two consecutive conformational search cycles. Afterwards, for chemical shift calculations, all resulting conformers were subjected to geometry optimization using B3LYP/6-311+G(2d,p) level of theory in gas-phase, and shielding tensors were then computed at mPW1PW91/6-311+G(2d,p) level of theory with polarizable continuum model (PCM). After dereplication, resulting isotropic shielding values were scaled based on slopes and intercepts provided by the CHESHIRE website (http://cheshirenmr.info) (for ^{1}H nuclei, slope = -1.0933 and intercept = 31.9088; for ^{13}C nuclei, slope = -1.0449 and intercept = 187.1018). Geometry optimization, frequencies and shielding tensor calculations were carried out with the Gaussian16 package (Frisch et al., 2016). Boltzmann distributions were estimated from the B3LYP/6-311+G(2d,p) level of theory using the sum of electronic and thermal free energies at 298.15 K. Only conformers with energies within 2.5 kcal mol^{-1} from the global minimum were submitted to the GIAO (Gauge-Independent Atomic Orbital) calculation. Avogadro 1.2.0 software was used for visualization of computed outputs.

4.5. Molecular networking and metabolomics analysis

All crude extracts and fractions mentioned in section 4.3 were profiled by UPLC-QTOF-MS and -MS/MS in positive ionization mode (MS scan range: 50-1500 *m/z*). The UPLC conditions were as follows: sample concentrations: 10 µg/mL and 1 µg/mL in 80% MeOH, injection volume: 5 µL, mobile phase solvent A: H_2O/FA (100:0.1, v/v) and solvent B: ACN/FA (100:0.1, v/v), and gradient: 0-2 min (2% B), 22-24 min

(100% B), 25-27 min (2% B). Raw data obtained from the UPLC-QTOF-MS/MS analysis were converted to *abf format using the Analysis Base File converter. Then, data processing was carried out with MS-Dial (Tsugawa et al., 2015), followed by the development of a feature-based molecular network, using the GNPS platform. The MS data processing workflow of MS-Dial (version 4.24) comprises *abf file import, data collection, peak detection, MS2 deconvolution, ion and adduct definition, peak alignment and isotope tracking. All MS data of the crude extracts and fractions were combined, in order to create a single molecular network. Setting parameters were as follows: positive ionization mode, centroid data, time analysis: 0.5-27.0 min, MS1 and MS2 mass range: 50-1500 Da, MS1 tolerance: 0.01 Da, MS2 tolerance: 0.025 Da, peak detection limit: 30,000, mass slice width: 0.1, MS/MS abundance cut off: 100 amplitude, ion and adducts: $[M]^+$, $[M+H]^+$, $[M+Na]^+$. Afterwards, processed files including an *mgf file and a text table were uploaded to the GNPS website and a molecular network was created with the feature-based molecular networking workflow (Nothias et al., 2019; Wang et al., 2016). To visualize the network, the output was imported into Cytoscape version 3.8.0 (Shannon et al., 2003). Peak annotation was performed manually for known compounds isolated by the authors and/or previously reported in literature. Due to co-elution, typical fragments of tentatively identified compounds were confirmed by MRM (multiple-reaction monitoring), conducted with the UPLC-TQD-MS system and using the LC conditions described in the section 4.3 and the MS setting parameters as demonstrated in Fig. 5.

Declaration of competing interest

The authors declare no conflicts of interest.

Acknowledgements

The authors are grateful to Prof. Herrebout for sharing the Gaussian16 software. The computational resources and services used in this work were provided by the HPC core facility CalcUA of the University of Antwerp, and VSC (Flemish Supercomputer Center), funded by the Research Foundation - Flanders (FWO) and the Flemish Government. Also, I would like to express special thanks to Daniel Méndez-Gonzales for his aid in the molecular networking analysis (Chemistry Department, Faculty of Applied Sciences, University of Camagüey, Cuba).

Author contributions

Hien T. N. Le: performing all experiments and writing the manuscript; E. Van Roy and E. Dendooven: performing part of the isolation work; L. Peeters: MS data analysis; Dr. M. Theunis, Dr. K. Foubert, Prof. L. Pieters, Dr. E. Tuenter: supervision, conceptualization, discussion, data analysis, writing and revision of the manuscript.

References

Beharry, S., Heinrich, M., 2018. Is the hype around the reproductive health claims of maca (*Lepidium meyenii* Walp.) J. Ethnopharmacol. 211, 126–170.https://doi.org/https://doi.org/10.1016/j.jep.2017.08.003

Cao, R., Peng, W., Wang, Z., Xu, A., 2007. Carboline Alkaloids: Biochemical and Pharmacological Functions. Curr. Med. Chem. 14, 479–500. https://doi.org/10.2174/092986707779940998

Carvalho, F. V., Ribeiro, P.R., 2019. Structural diversity, biosynthetic aspects, and LC-HRMS data compilation for the identification of bioactive compounds of *Lepidium meyenii*. Food Res. Int. 125, 108615. https://doi.org/10.1016/j.foodres.2019.108615

Cheng, C., Shen, F., Ding, G., Liu, A., Chu, S., Ma, Y., Hou, X., Hao, E., Wang, X., Yuanyuan Hou Y., Bai, G., 2020. Lepidiline A improves the balance of endogenous sex hormones and increases fecundity by Targeting HSD17B1. Mol. Nutr. Food Res. 64, 1900706. https://doi.org/10.1002/mnfr.201900706

Cui, B., Zheng, B., He, K.L., Zheng, Q., 2003. Imidazole alkaloids from *Lepidium meyenii*. J. Nat. Prod. 66, 1101–1103. https://doi.org/10.1021/np030031i

Ermanis, K., Parkes, K., Agback, T., Goodman, J., 2017. Doubling the power of DP4 for computational structure elucidation. Org. Biomol. Chem. 15. https://doi.org/10.1039/C7OB01379E

Ganzera, M., Zhao, J., Muhammad, I., Khan, I.A., 2002. Chemical profiling and standardization of *Lepidium meyenii* (Maca) by reversed phase high performance liquid chromatography. Chem. Pharm. Bull. 50, 988–991. https://doi.org/10.1248/cpb.50.988

Gaussian 16, Revision A.03, M. J. Frisch, G. W. Trucks, H. B. Schlegel, G. E. Scuseria, M. A. Robb, J. R. Cheeseman, G. Scalmani, V. Barone, G. A. Petersson, H. Nakatsuji, X. Li, M. Caricato, A. V. Marenich, J. Bloino, B. G. Janesko, R. Gomperts, B. Mennucci, H. P. Hratchian, J. V. Ortiz, A. F. Izmaylov, J. L. Sonnenberg, D. Williams-Young, F. Ding, F. Lipparini, F. Egidi, J. Goings, B. Peng, A. Petrone, T. Henderson, D. Ranasinghe, V. G. Zakrzewski, J. Gao, N. Rega, G. Zheng, W. Liang, M. Hada, M. Ehara, K. Toyota, R. Fukuda, J. Hasegawa, M. Ishida, T. Nakajima, Y. Honda, O. Kitao, H. Nakai, T. Vreven, K. Throssell, J. A. Montgomery, Jr., J. E. Peralta, F. Ogliaro, M. J. Bearpark, J. J. Heyd, E. N. Brothers, K. N. Kudin, V. N. Staroverov, T. A. Keith, R. Kobayashi, J. Normand, K. Raghavachari, A. P. Rendell, J. C. Burant, S. S. Iyengar, J. Tomasi, M. Cossi, J. M. Millam, M. Klene, C. Adamo, R. Cammi, J. W. Ochterski, R. L. Martin, K. Morokuma, O. Farkas, J. B. Foresman, and D. J. Fox, Gaussian, Inc., Wallingford CT, 2016.

Geng, P., Sun, J., Chen, P., Brand, E., Frame, J., Meissner, H., Stewart, J., Gafner, S., Clark, S., Miller, J., Harnly, J., 2020. Characterization of Maca (*Lepidium meyenii/Lepidium peruvianum*) using a mass spectral fingerprinting, metabolomic analysis, and genetic sequencing approach. Planta Med. 86. https://doi.org/10.1055/a-1161-0372

Gutsche, B., Herderich, M., 1997. HPLC-MS/MS profiling of tryptophan-derived alkaloids in food: identification of tetrahydro-β-carbolinedicarboxylic acids. J. Agric. Food Chem. 45, 2458–2462. https://doi.org/10.1021/jf960952h

Geng, H.C., Yang, D.S., Chen, X.L., Wang, L.X., Zhou, M., Mei, W.Q., 2018. Meyeniihydantoins A–C, three novel hydantoin derivatives from the roots of Lepidium meyenii Walp. Phytochem. Lett. 26, 208–211. https://doi.org/10.1016/j.phytol.2018.06.010

Huang, Y.-J., Peng, X.-R., Qiu, M.-H., 2018. Progress on the Chemical Constituents Derived from Glucosinolates in Maca (Lepidium meyenii). Nat. Products Bioprospect. 8, 405–412. https://doi.org/10.1007/s13659-018-0185-7

Jensen, F., 2008. Basis set convergence of nuclear magnetic shielding constants calculated by density functional methods. J. Chem. Theory Comput. J. Chem. Theory Comput. 2008, 4, 5, 719–727 https://doi.org/10.1021/ct800013z

Jin, W., Chen, X., Dai, P., Yu, L., 2016. Lepidiline C and D: two new imidazole alkaloids from *Lepidium meyenii* Walpers (Brassicaceae) roots. Phytochem. Lett. 17, 158–161. https://doi.org/https://doi.org/10.1016/j.phytol.2016.07.001

Kitamura, S., Morisseau, C., Harris, T.R., Inceoglu, B., Hammock, B.D., 2017. Occurrence of urea-based soluble epoxide hydrolase inhibitors from the plants in the order Brassicales. PLoS One 12, 4–9. https://doi.org/10.1371/journal.pone.0176571

Lodewyk, M.W., Siebert, M.R., Tantillo, D.J., 2012. Computational prediction of ^{1}H and ^{13}C chemical shifts: a useful tool for natural product, mechanistic, and synthetic organic chemistry. Chem. Rev. 112, 1839–1862. https://doi.org/10.1021/cr200106v

Maccallini, C., Montagnani, M., Paciotti, R., Ammazzalorso, A., De Filippis, B., Di Matteo, M., Di Silvestre, S., Fantacuzzi, M., Giampietro, L., Potenza, M.A., Re, N., Pandolfi, A., Amoroso, R., 2015. Selective acetamidine-based nitric oxide synthase inhibitors: synthesis, docking, and biological studies. ACS Med. Chem. Lett. 6, 635–640. https://doi.org/10.1021/acsmedchemlett.5b00149

Minkin, V., Mikhailov, I., 2010. Amidines and imidates: Volume 2 (1991), in: Cheminform. pp. 527–621. https://doi.org/10.1002/9780470772478.ch11

Muhammad, I., Zhao, J., Dunbar, D.C., Khan, I.A., 2002. Constituents of *Lepidium meyenii* 'maca.' Phytochemistry 59, 105–110. https://doi.org/https://doi.org/10.1016/S0031-9422(01)00395-8

Nothias, L.F., Petras, D., Schmid, R., Dührkop, K., Rainer, J., Sarvepalli, A., Protsyuk, I., Ernst, M., Tsugawa, H., Fleischauer, M., Aicheler, F., Aksenov, A., Alka, O., Allard, P.-M., Barsch, A., Cachet, X., Caraballo, M., Da Silva, R.R., Dang, T., Garg, N., Gauglitz, J.M., Gurevich, A., Isaac, G., Jarmusch, A.K., Kameník, Z., Kang, K. Bin, Kessler, N., Koester, I., Korf, A., Gouellec, A. Le, Ludwig, M., Christian, M.H., McCall, L.-I., McSayles, J., Meyer, S.W., Mohimani, H., Morsy, M.,

Moyne, O., Neumann, S., Neuweger, H., Nguyen, N.H., Nothias-Esposito, M., Paolini, J., Phelan, V. V, Pluskal, T., Quinn, R.A., Rogers, S., Shrestha, B., Tripathi, A., van der Hooft, J.J.J., Vargas, F., Weldon, K.C., Witting, M., Yang, H., Zhang, Z., Zubeil, F., Kohlbacher, O., Böcker, S., Alexandrov, T., Bandeira, N., Wang, M., Dorrestein, P.C., 2019. Feature-based molecular networking in the GNPS analysis environment. bioRxiv 812404. https://doi.org/10.1101/812404

Shannon, P., Markiel, A., Ozier, O., Baliga, N.S., Wang, J.T., Ramage, D., Amin, N., Schwikowski, B., Ideker, T., 2003. Cytoscape: a software environment for integrated models of biomolecular interaction networks. Genome Res. 13, 2498–2504. https://doi.org/10.1101/gr.1239303

Tian, X.X., Peng, X.R., Yu, M.Y., Huang, Y.J., Wang, X., Zhou, L., Qiu, M., 2018. Hydantoin and thioamide analogues from Lepidium meyenii. Phytochem. Lett. 25, 70–73. https://doi.org/10.1016/j.phytol.2018.03.011

Tsugawa, H., Cajka, T., Kind, T., Ma, Y., Higgins, B., Ikeda, K., Kanazawa, M., VanderGheynst, J., Fiehn, O., Arita, M., 2015. MS-DIAL: data-independent MS/MS deconvolution for comprehensive metabolome analysis. Nat. Methods 12, 523–526. https://doi.org/10.1038/nmeth.3393

Wang, M., Carver, J.J., Phelan, V. V, Sanchez, L.M., Garg, N., Peng, Y., Nguyen, D.D., Watrous, J., Kapono, C.A., Luzzatto-Knaan, T., Porto, C., Bouslimani, A., Melnik, A. V, Meehan, M.J., Liu, W.-T., Crüsemann, M., Boudreau, P.D., Esquenazi, E., Sandoval-Calderón, M., Kersten, R.D., Pace, L.A., Quinn, R.A., Duncan, K.R., Hsu, C.-C., Floros, D.J., Gavilan, R.G., Kleigrewe, K., Northen, T., Dutton, R.J., Parrot, D., Carlson, E.E., Aigle, B., Michelsen, C.F., Jelsbak, L., Sohlenkamp, C., Pevzner, P., Edlund, A., McLean, J., Piel, J., Murphy, B.T., Gerwick, L., Liaw, C.-C., Yang, Y.-L., Humpf, H.-U., Maansson, M., Keyzers, R.A., Sims, A.C., Johnson, A.R., Sidebottom, A.M., Sedio, B.E., Klitgaard, A., Larson, C.B., Boya P, C.A., Torres-Mendoza, D., Gonzalez, D.J., Silva, D.B., Marques, L.M., Demarque, D.P., Pociute, E., O'Neill, E.C., Briand, E., Helfrich, E.J.N., Granatosky, E.A., Glukhov, E., Ryffel, F., Houson, H., Mohimani, H., Kharbush, J.J., Zeng, Y., Vorholt, J.A., Kurita, K.L., Charusanti, P., McPhail, K.L., Nielsen, K.F., Vuong, L., Elfeki, M., Traxler, M.F., Engene, N., Koyama, N., Vining, O.B., Baric, R., Silva, R.R., Mascuch, S.J., Tomasi, S., Jenkins, S., Macherla, V., Hoffman, T., Agarwal, V., Williams, P.G., Dai, J., Neupane, R., Gurr, J., Rodríguez, A.M.C., Lamsa, A., Zhang, C., Dorrestein, K., Duggan, B.M., Almaliti, J., Allard, P.-M., Phapale, P., Nothias, L.-F., Alexandrov, T., Litaudon, M., Wolfender, J.-L., Kyle, J.E., Metz, T.O., Peryea, T., Nguyen, D.-T., VanLeer, D., Shinn, P., Jadhav, A., Müller, R., Waters, K.M., Shi, W., Liu, X., Zhang, L., Knight, R., Jensen, P.R., Palsson, B.Ø., Pogliano, K., Linington, R.G., Gutiérrez, M., Lopes, N.P., Gerwick, W.H., Moore, B.S., Dorrestein, P.C., Bandeira, N., 2016. Sharing and community curation of mass spectrometry data with Global Natural Products Social Molecular Networking. Nat. Biotechnol. 34, 828–837. https://doi.org/10.1038/nbt.3597

Yu, M.Y., Qin, X.J., Peng, X.R., Wang, X., Tian, X.X., Li, Z.R., Qiu, M.H., 2017. Macathiohydantoins B–K, novel thiohydantoin derivatives from Lepidium meyenii. Tetrahedron 73, 4392–4397. https://doi.org/10.1016/j.tet.2017.05.096

Zhou, M., Zhang, R.-Q., Chen, Y.-J., Liao, L.-M., Sun, Y.-Q., Ma, Z.-H., Yang, Q.-F., Li, P., Ye, Y.-Q., Hu, Q.-F., 2018. Three new pyrrole alkaloids from the roots of *Lepidium meyenii*. Phytochem. Lett. 23, 137–140. https://doi.org/https://doi.org/10.1016/j.phytol.2017.12.002

Zhou, M., Ma, H.Y., Xing, H.H., Li, P., Li, G.P., Geng, H.C., Hu, Q.F., Yang, G.Y., 2017. Biomimetic synthesis of macahydantoins A and B from *Lepidium meyenii*, and structure revision of macahydantoin B as a class of thiohydantoin with a 4-methyl-hexahydropyrrolo[1,2-c]imidazole skeleton. Org. Lett. 19, 4952–4955. https://doi.org/10.1021/acs.orglett.7b02433

Zhou, Y., Li, P., Brantner, A., Wang, H., Shu, X., Yang, J., Si, N., Han, L., Zhao, H., Bian, B., 2017. Chemical profiling analysis of Maca using UHPLC-ESI-Orbitrap MS coupled with UHPLC-ESI-QqQ MS and the neuroprotective study on its active ingredients. Sci. Rep. 7, 44660. https://doi.org/10.1038/srep44660

FIGURES

Fig. 1. Structure of isolated imidazole, amidine and *β*-carboline alkaloids

Fig. 2. Key COSY and HMBC correlations observed for lepidiline E (**1**) F (**2**) and G (**3**)

Fig. 3. Structures of the proposed 'macaridine' (left) and macapyrrolin C (right)

Fig. 4. Cluster containing identified imidazole and amidine alkaloids. Nodes were numbered from lowest to highest *m/z* values. Detailed information on unknown nodes can be found as Supporting Information.

Fig. 5. Results of three channel MRM scans using UPLC conditions for the TQD system.

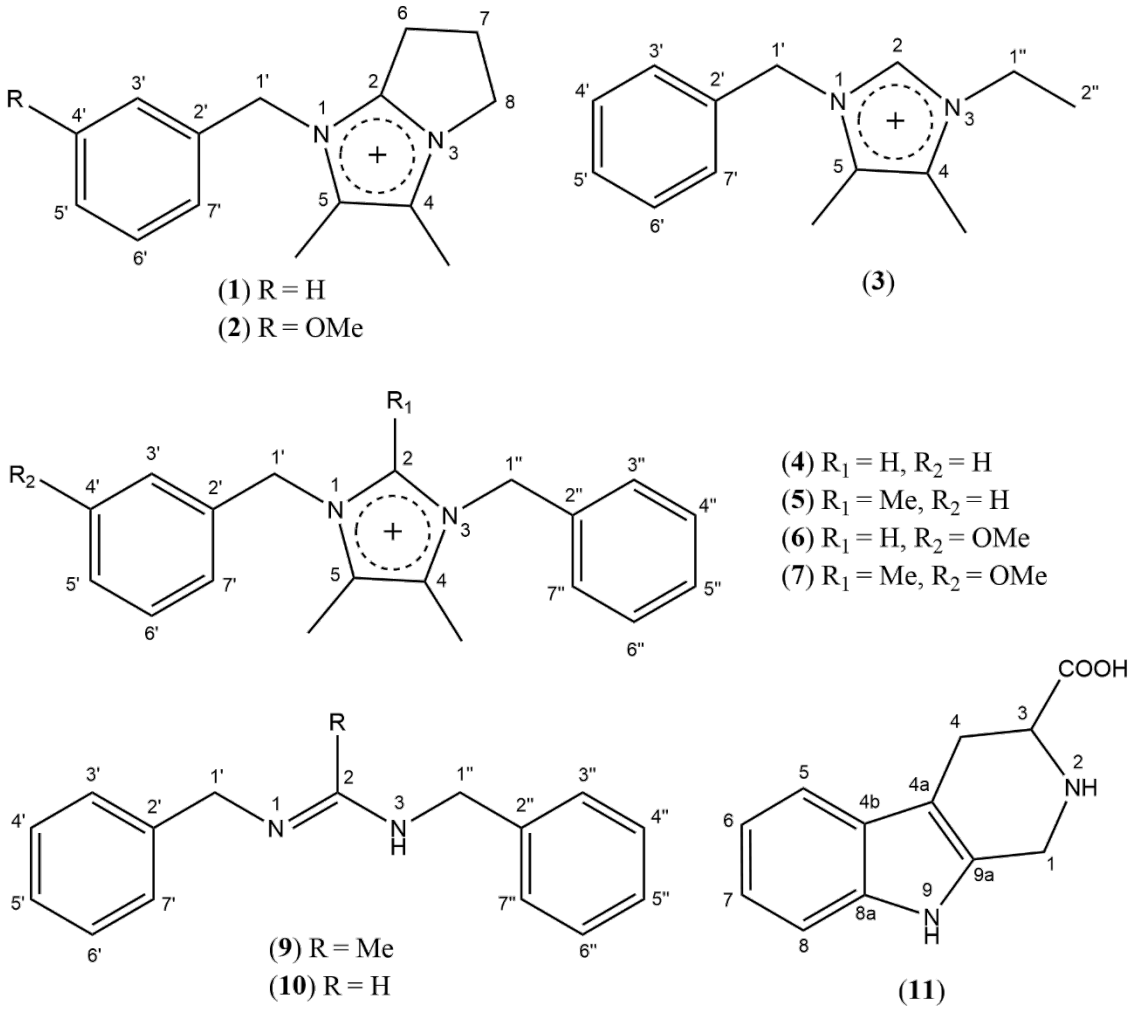

Fig. 1. Structure of isolated imidazole, amidine and *β*-carboline alkaloids

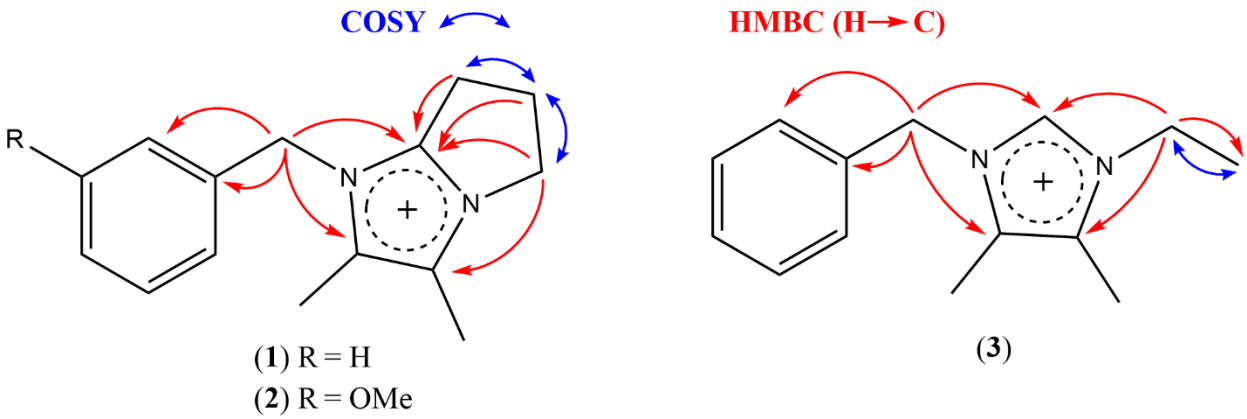

(**1**) R = H
(**2**) R = OMe

(**3**)

Fig. 2. Key COSY and HMBC correlations observed for lepidiline E (**1**) F (**2**) and G (**3**)

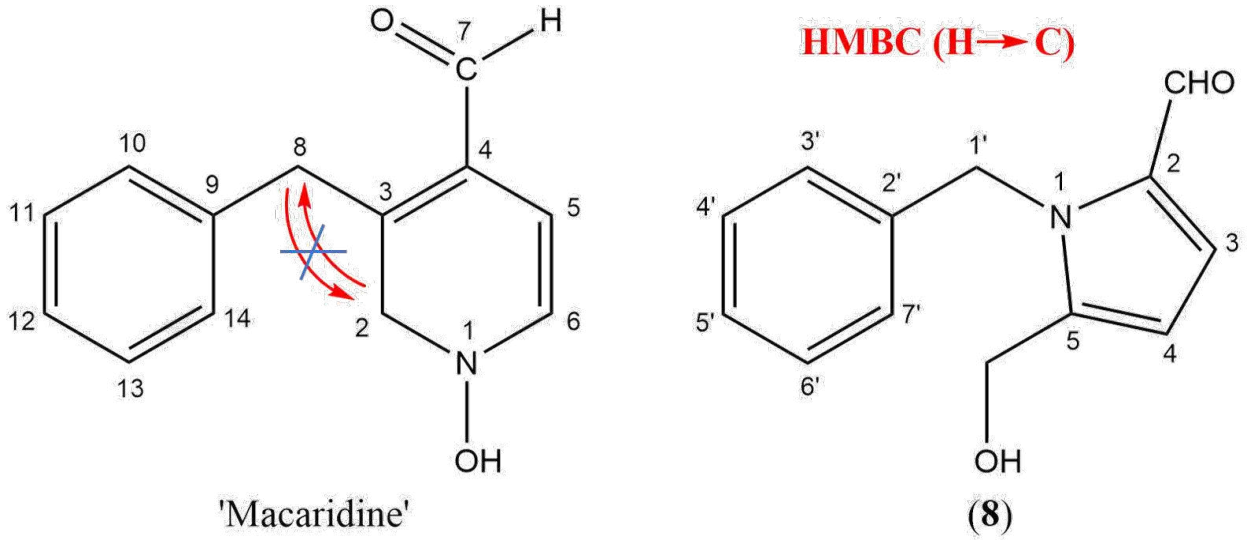

'Macaridine'

(**8**)

Fig. 3. Structures of the proposed ‘macaridine’ (left) and macapyrrolin C (right)

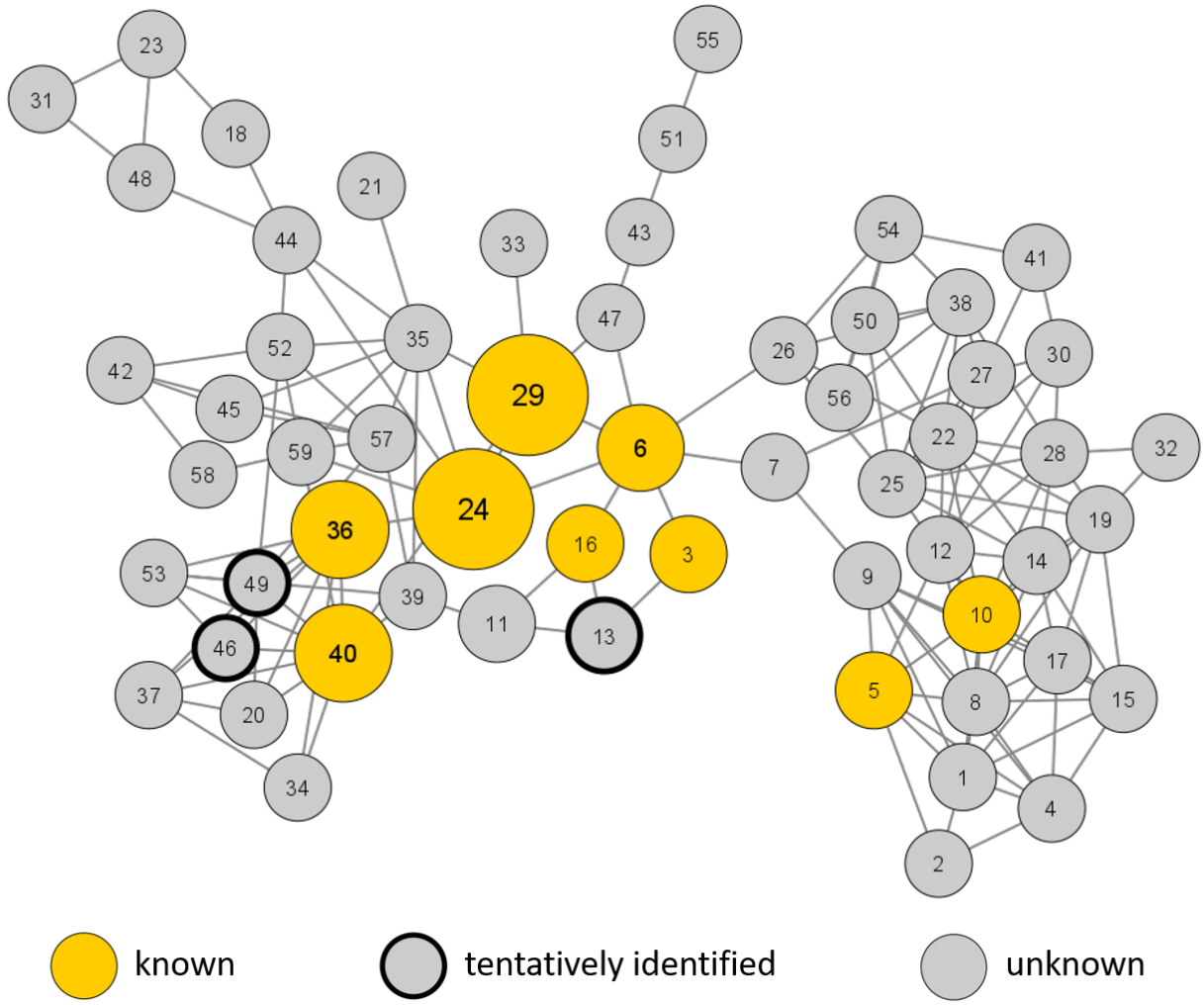

Fig. 4. Cluster containing identified imidazole and amidine alkaloids. Nodes were numbered from lowest to highest *m/z* values. Detailed information on unknown nodes can be found as Supporting Information.

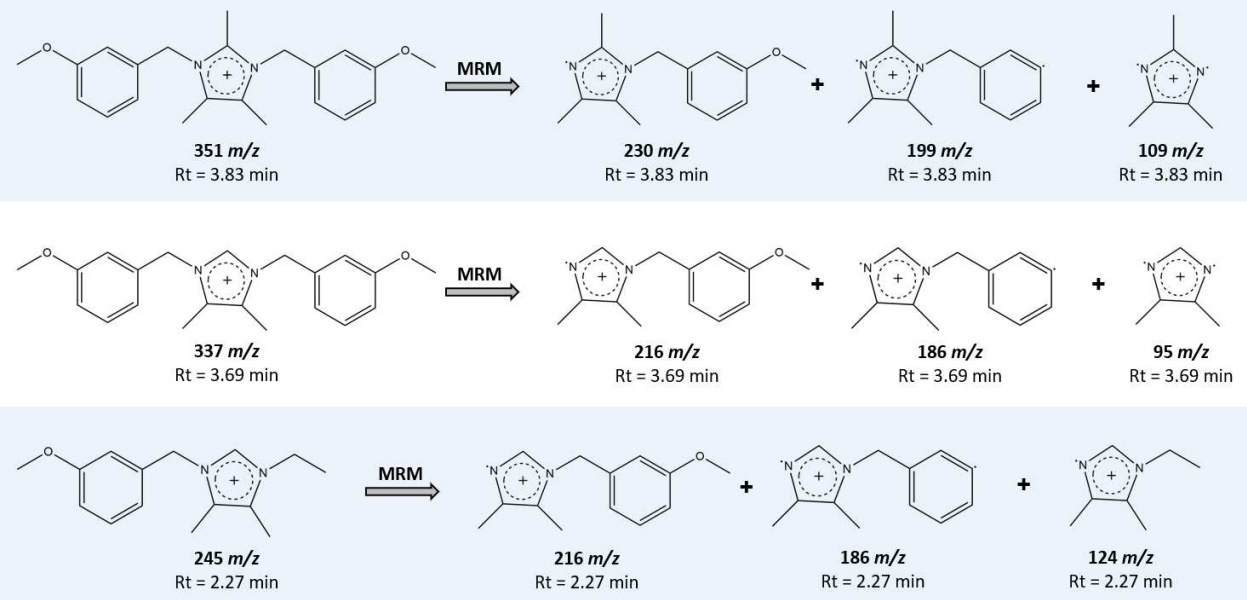

Fig. 5. Results of three channel MRM scans using UPLC conditions for the TQD system.

Table 1. ^{1}H and ^{13}C NMR assignments of compounds **1** – **3** (lepidilines E, F and G), recorded in CD_3OD

Position	Compound **1**		Compound **2**		Compound **3**	
	δ_H (mult., *J* in Hz)	δ_C	δ_H (mult., *J* in Hz)	δ_C	δ_H (mult., *J* in Hz)	δ_C
1	-	-	-	-	-	-
2	-	151.6	-	151.6	n.o.	134.5
3	-	-	-	-	-	-
4	-	124.9	-	124.6	-	128.9
5	-	131.1	-	131.1	-	128.7
6	3.08 (t, 7.6)	24.5	3.08 (t, 7.6)	24.4	-	-
7	2.75 (quintet, 7.5)	26.1	2.75 (quintet, 7.4)	25.9	-	-
8	4.20 (t, 7.4)	47.2	4.19 (t, 7.4)	46.9	-	-
1’	5.29 (s)	50.6	5.26 (s)	50.2	5.37 (s)	51.5
2’	-	135.1	-	135.8	-	135.1
3’	7.28 *	128.6	6.83 *	114.4	7.30 *	128.7
4’	7.39-7.45 *	130.4	-	161.5	7.37-7.46 *	130.4
5’	7.39-7.45 *	129.9	6.97 (dd; 8.2, 2.2)	114.6	7.37-7.46 *	129.9
6’	7.39-7.45 *	130.4	7.34 (t, 8.0)	131.3	7.37-7.46 *	130.4
7’	7.28 *	128.6	6.81 *	120.4	7.30 *	128.7
1’’	-	-	-	-	4.20 *	43.4
2’’	-	-	-	-	1.52 (t, 7.35)	15.0
4-Me	2.25 (s)	8.1	2.25 (s)	7.8	2.31 (s)	8.0
5-Me	2.19 (s)	8.8	2.19 (s)	8.6	2.19 (s)	8.4
4’-OMe	-	-	3.81	55.5	-	-

* overlapping signals; n.o.: not observed

Table 2. ^{1}H and ^{13}C NMR assignments of compounds **9** and **10** recorded in $CDCl_3$

Position	Compound **9**		Compound **10**			
	Major isomer		Major isomer		Minor isomer	
	δ_H (mult., *J* in Hz)	δ_C	δ_H (mult., *J* in Hz)	δ_C	δ_H (mult., *J* in Hz)	δ_C
1	-	-	-	-	-	-
2	-	168.0	7.28-7.38 *	168.7	7.28-7.38 *	166.3
3	11.00 (brs)	-	10.89 (brs)	-	8.79 (brs)	-
1’	4.52 (s)	47.2	4.50 (s)	46.7	4.65 (s)	46.9
2’	-	135.0	-	135.1	-	133.9
3’	7.31 *	126.7	7.27 *	127.1	7.26 *	127.9
4’	7.35-7.40 *	129.2	7.28-7.38 *	129.0	7.28-7.38 *	129.0
5’	7.35-7.40 *	128.3	7.28-7.38 *	129.0	7.28-7.38 *	129.0
6’	7.35-7.40 *	129.2	7.28-7.38 *	129.0	7.28-7.38 *	129.0
7’	7.31 *	126.7	7.27	127.1	7.26 *	127.9
1”	4.53 (s)	47.2	3.78 (s)	36.2	4.07 (s)	38.7
2”	-	135.0	-	129.9	-	131.5
3”	7.31 *	126.7	7.17	129.1	7.34-7.39 *	129.5
4”	7.35-7.40 *	129.2	7.28-7.38 *	129.0	7.28-7.38 *	129.0
5”	7.35-7.40 *	128.3	7.28-7.38 *	129.0	7.28-7.38 *	129.0
6”	7.35-7.40 *	129.2	7.28-7.38 *	129.0	7.28-7.38 *	129.0
7”	7.31 *	126.7	7.17	129.1	7.34-7.39 *	129.5
2-Me	2.04 (s)	13.07	-	-	-	-

* overlapping signals

Table 3. Comparison between experimental (exp) and calculated (calc) ^{1}H and ^{13}C NMR chemical shifts of 'macaridine' and macapyrrolin C

Position	Macaridine in $CDCl_3$ (Muhammad et al. 2001)				Position	Macapyrrolin C in $CDCl_3$ (current study)			
	δ_H (exp)	δ_H (calc)	δ_C (exp)	δ_C (calc)		δ_H (exp)	δ_H (calc)	δ_C (exp)	δ_C (calc)
1	-	-	-		1	-	-	-	-
8	5.73	3.82	48.9	35.9	1'	5.76	5.89	49.0	49.0
2	4.54	3.58	57.0	55.1	5-CH_2OH	4.57	4.12	57.1	57.3
6	6.29	6.19	111.2	94.5	4	6.32	6.08	111.2	110.7
5	6.94	5.33	124.8	126.1	3	6.96	6.69	124.7	124.2
10	6.98	7.15	126.5	127.6	3'	6.99	6.96	126.7	125.6
14	6.98	7.15	126.5	127.6	7'	6.99	6.96	126.7	125.6
12	7.22	7.18	128.0	128.1	5'	7.25	7.12	127.9	125.9
11	7.26	7.18	129.1	128.1	4'	7.29	7.17	129.3	127.5
13	7.26	7.18	129.1	130.8	6'	7.29	7.17	129.3	127.5
4	-	-	133.2	137.4	2	-	-	133.3	132.6
9	-	-	138.2	140.5	2'	-	-	138.3	137.9
3	-	-	142.5	151.6	5	-	-	142.3	143.0
7	9.52	9.69	180.2	184.6	2-CHO	9.57	9.26	180.2	177.9
CMAE		0.529		4.477	CMAE		0.183		1.008